Galaxy observations at radio wavelengths

A. Bosma
Observatoire de Marseille – LAM/OAMP

Link it to : galaxy formation problem
detailed structure of our Galaxy
problem of dark matter in galaxies

part I : some discussion about galaxy formation
part II : SKA and 21-cm HI rotation curves
part III: LOFAR and radio continuum in galaxies

- resolution is important
- SKA is fundamental for galaxies and cosmology
- LOFAR is a good pathway to SKA

Millenium Simulation

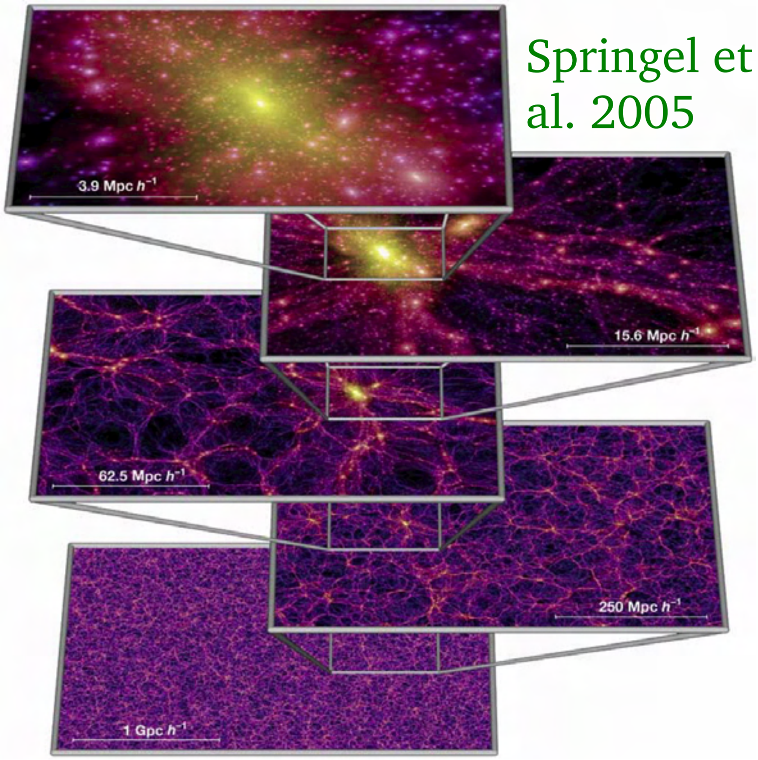

Springel et al. 2005

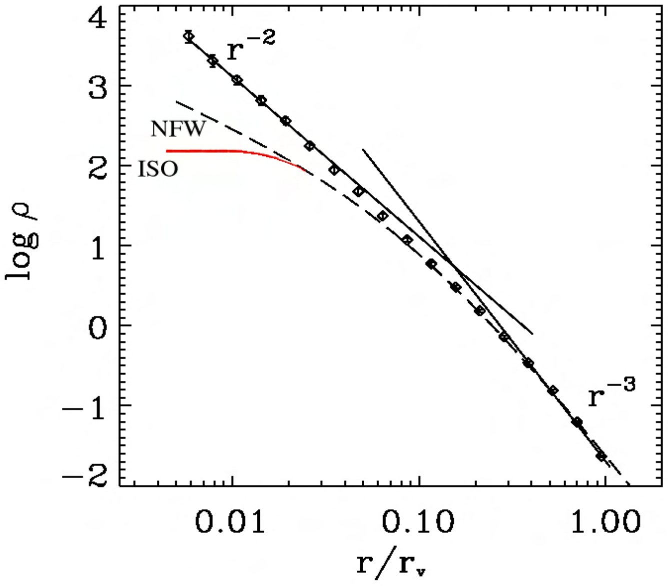

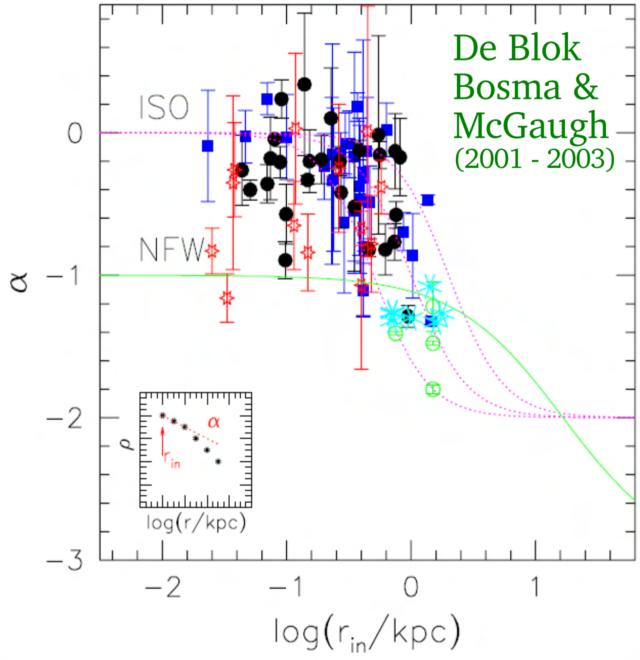

De Blok
Bosma &
McGaugh
(2001 - 2003)

ΛCDM has problems on galaxy scales

cuspy halos
lots of satellites

New 2-D data confirm the problem
Kuzio de Naray et al. 2006

Galaxy formation in ΛCDM

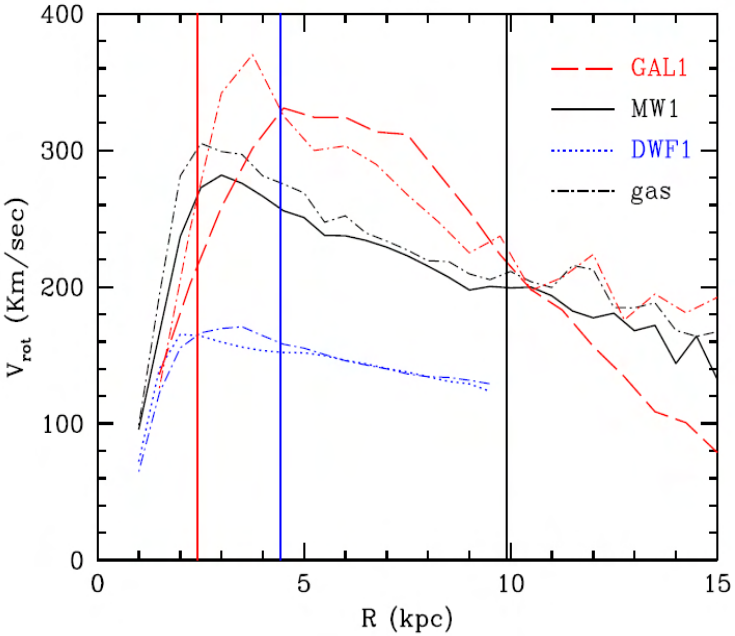

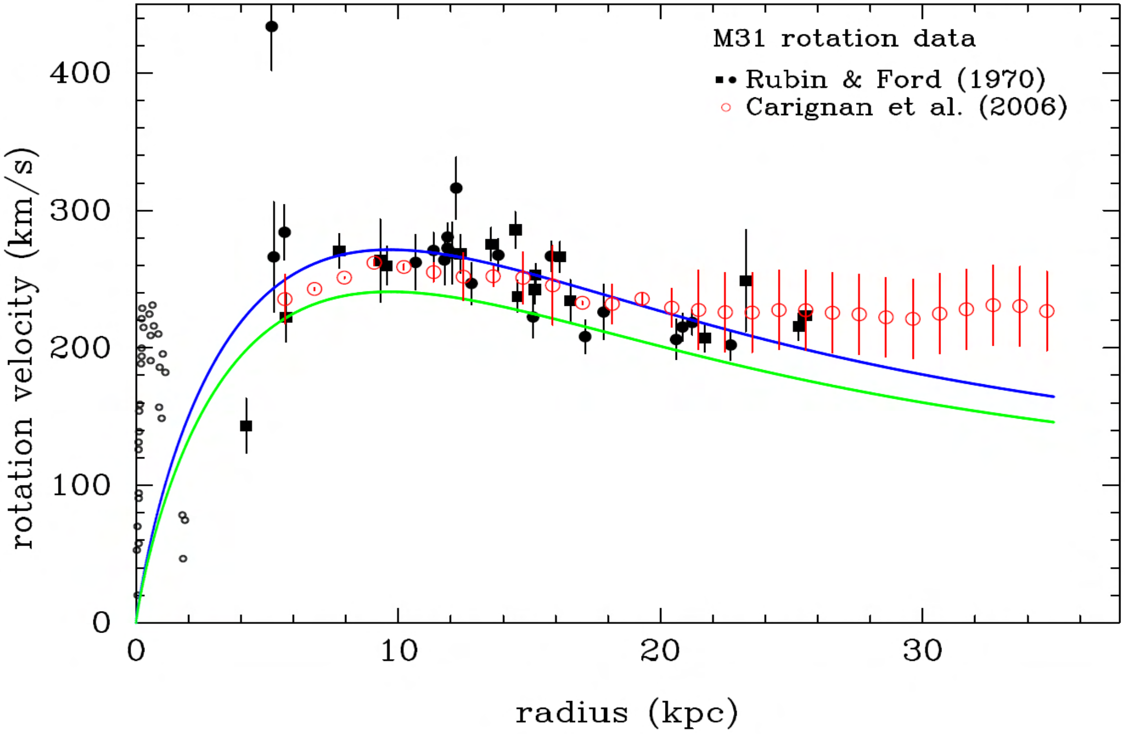

Feedback helps:

TF-relation zero point OK, but halos still too concentrated...

in fact there is a resolution problem

Governato et al. 2006

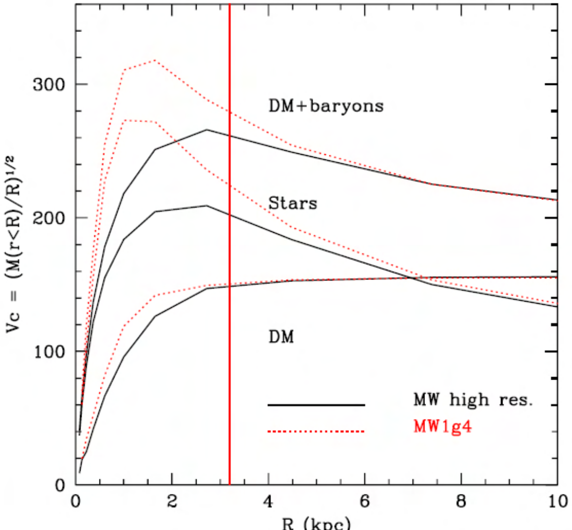

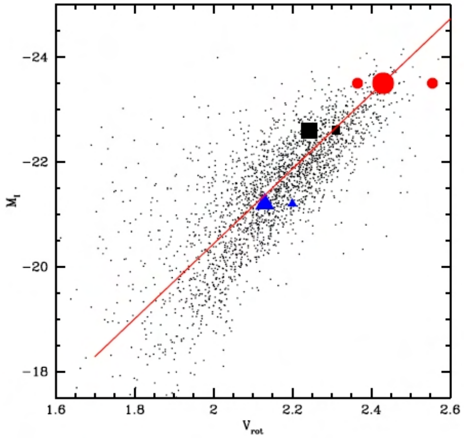

Star formation history and feedback

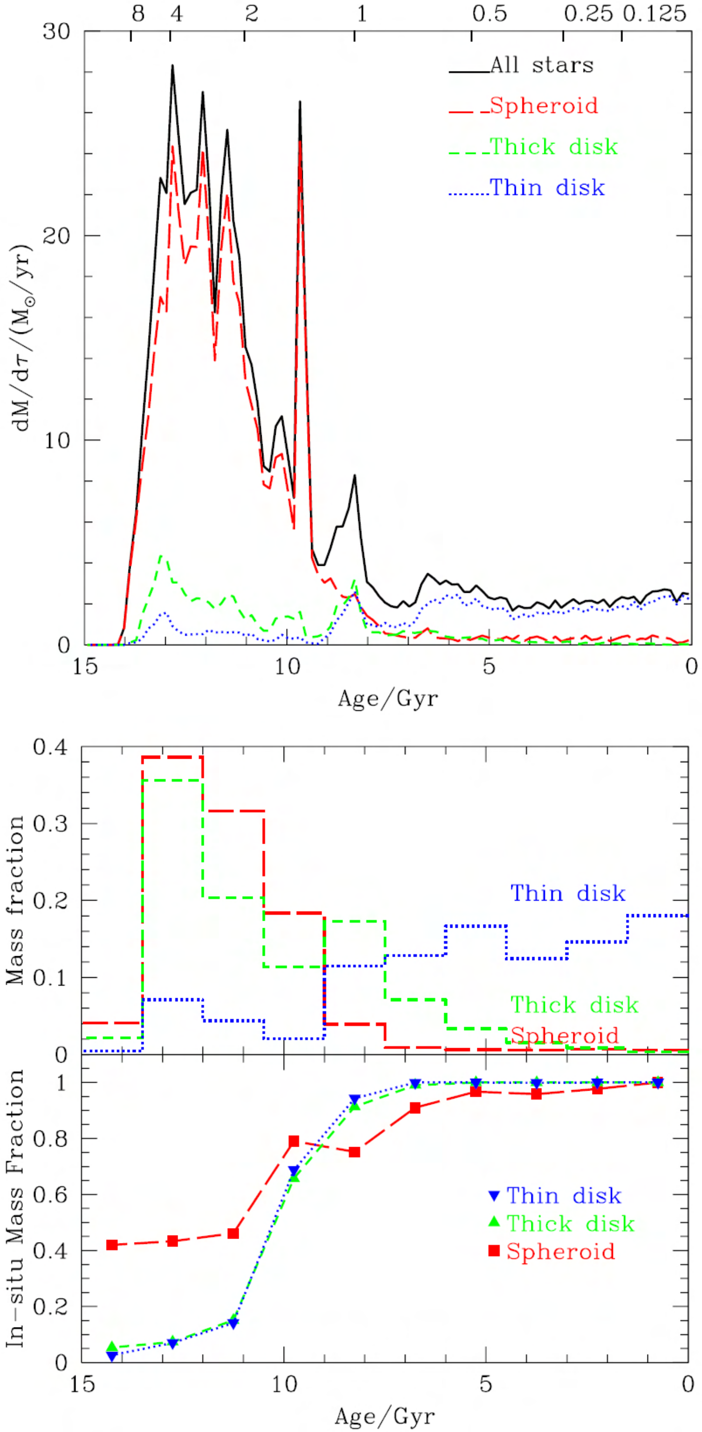

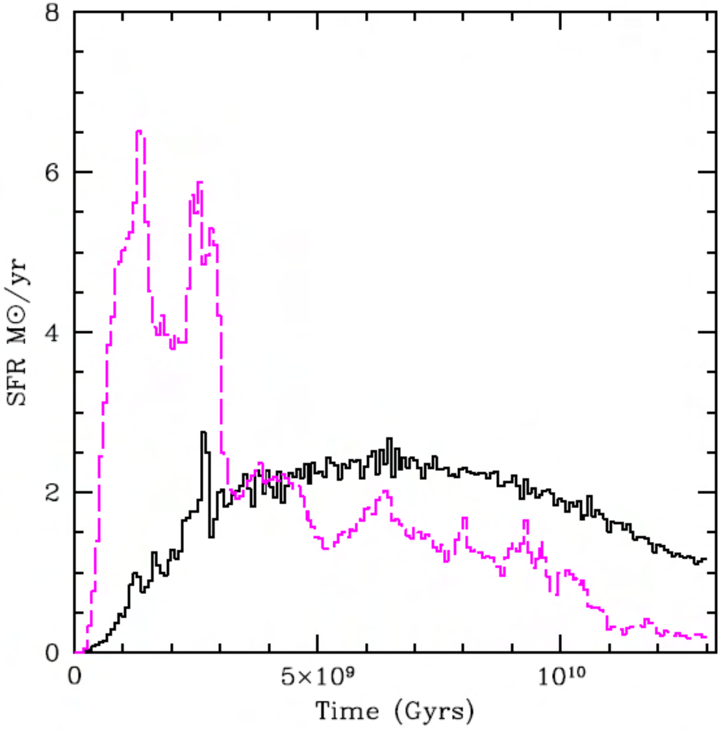

Figure 13. Galaxy DWF1: SFH including all stars within 4 R_z and R_d from the disk plane for two runs. Solid line: ϵSN=0.6, long dashed: no feedback, no UV. The addition of feedback smooths out the SF peaks otherwise present at high redshift and during the last major merger event at z=2.3. Feedback delays the conversion of gas into stars until gas accumulates and cools in the potential well of the main progenitor.

Abadi et al. 2003 Governato et al. 2006

Bar – Halo interaction

Athanassoula 2002, 2003

Mechanism is the exchange of angular momentum via the resonances

As a result, the mass concentration of the galaxy increases with time

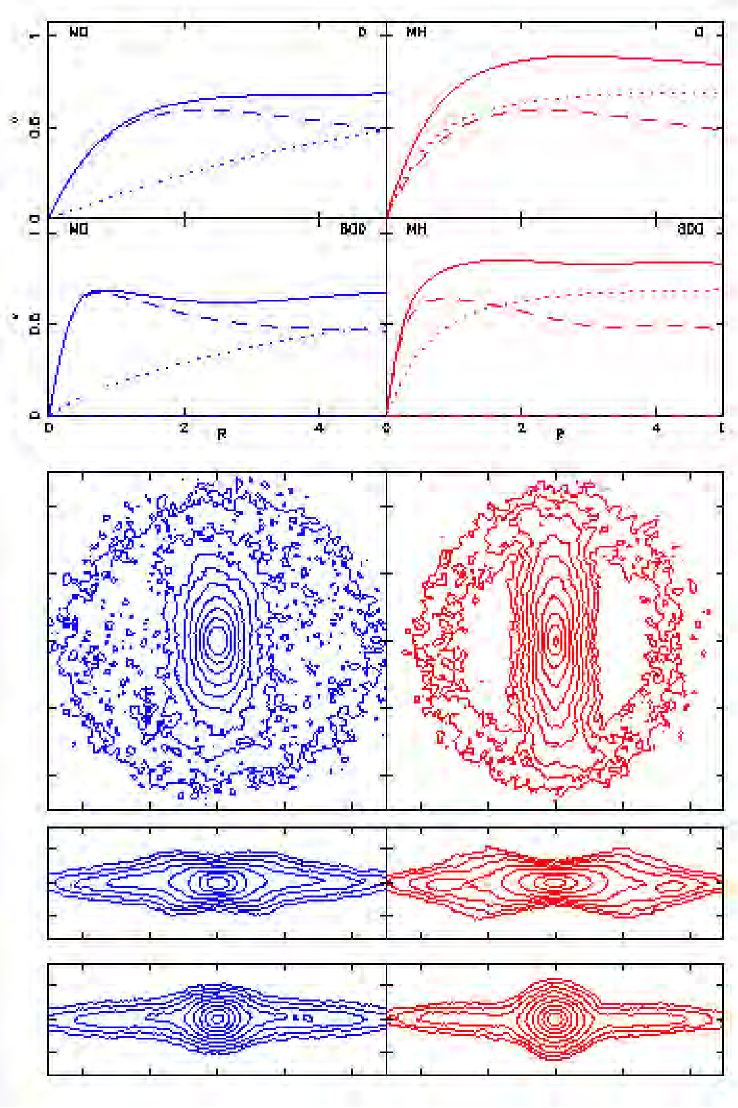

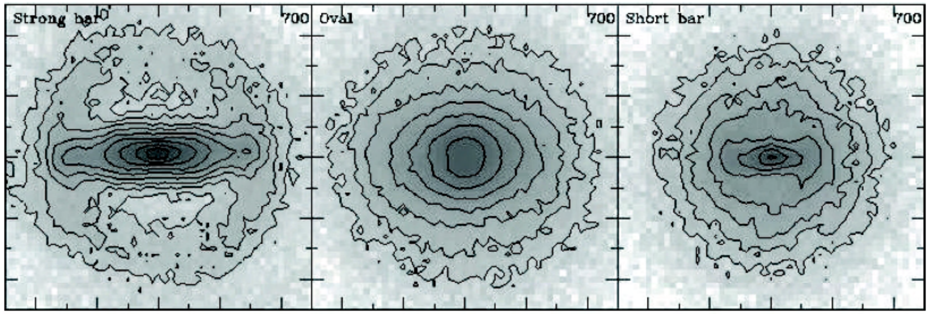

Considerable amount of angular momentum is exchanged

Little angular momentum exchanged

Responsive halo
Hot outer disc

Hot halo

Schematic evolution

One expects thus :

rapid evolution with a lot of merging at $z > 1.5 – 2$
slow evolution thereafter

in DM only simulations not much change of shape of RC
but in slow evolution simulations the galaxy concentrates

One way to test this is to use correlation of spiral arm pitch angle with shear rate (Segar et al. 2006), i.e.
morphology vs. redshift

Another is to collect rotation curves at larger z

Morphology vs. z

Bar fraction out to 8 Gyr lookback time Jogee et al. (2004)

Spiral arm pitch angle vs. shear rate Seigar et al. (2006)

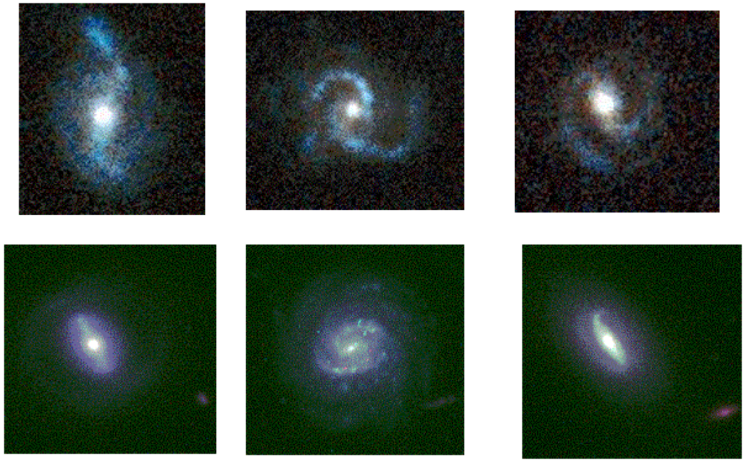

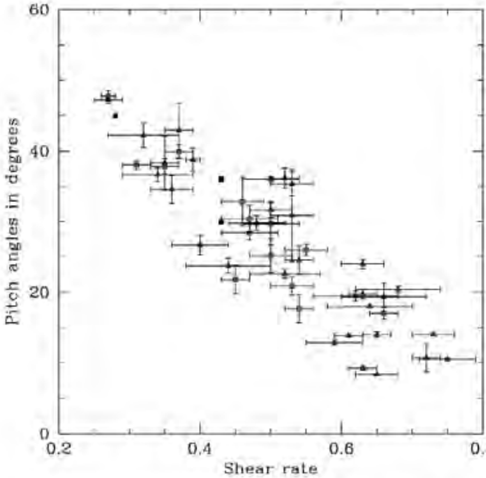

FIG. 3.— Spiral arm pitch angle versus rotation curve shear rate, showing a strong correlation. The solid squares represent galaxies with data measured by Block et al. (1999), the open squares are galaxies from Seigar et al. (2005), and the open triangles represent the data from the present sample.

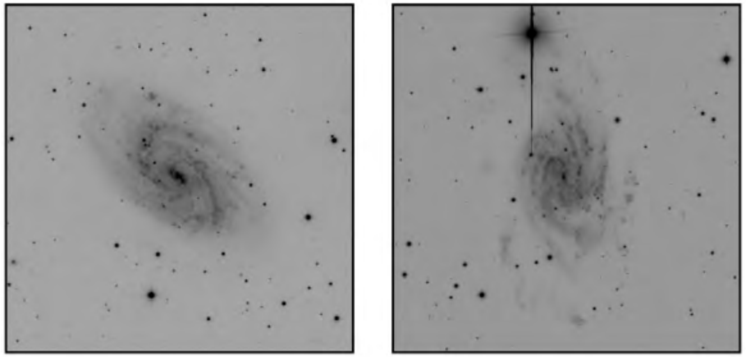

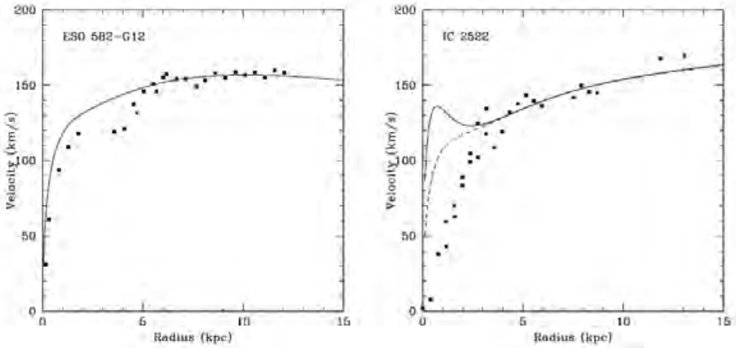

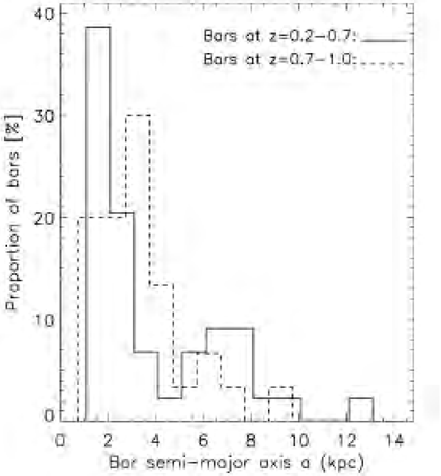

Quantitative interpretation of the rotation curves of spiral galaxies at redshifts $z \sim 0.7$ and $z \sim 1$

Fuchs et al. 2004, use a variation of Athanassoula et al. 1987

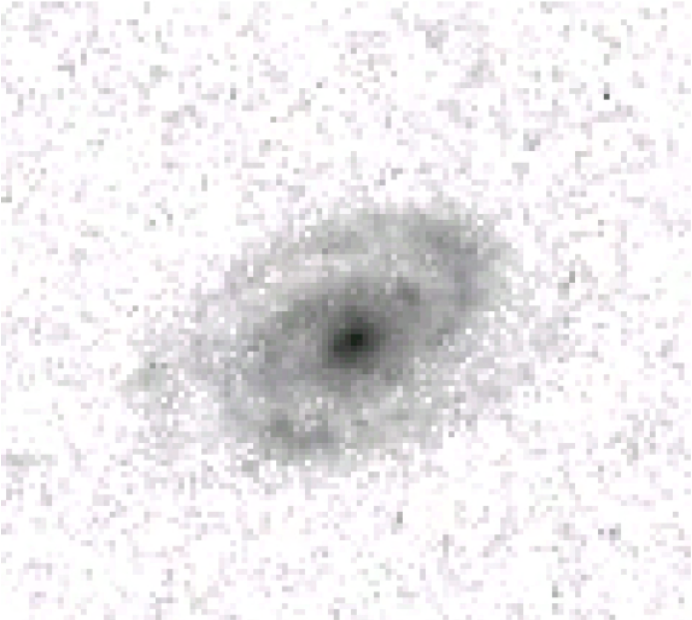

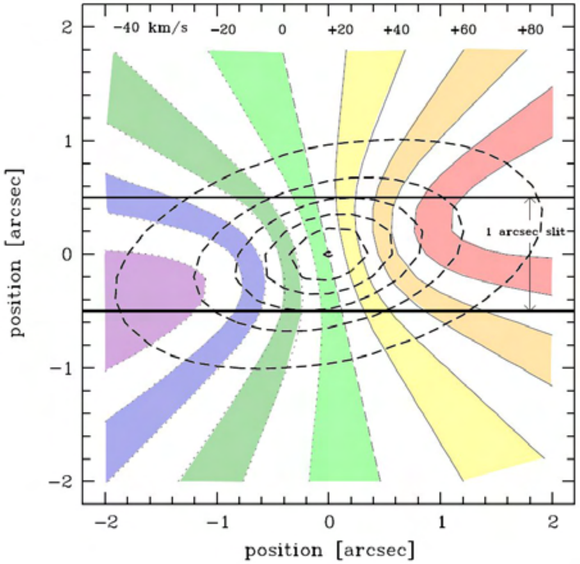

Strong spiral => Massive disk

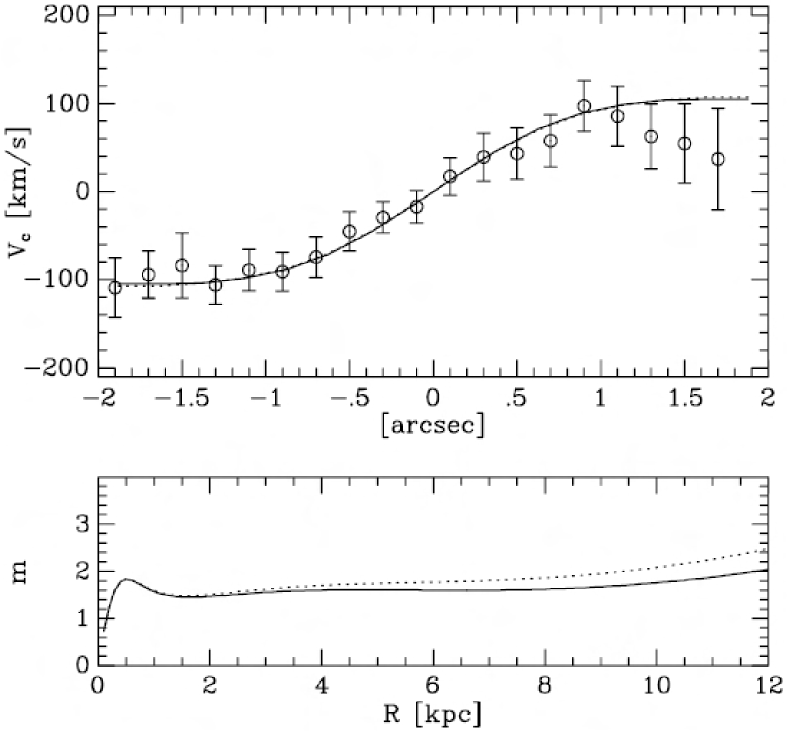

Fig. 3. *Upper panel*: model rotation curves of FDF 2484 fitted to the radial velocity data of Böhm et al. (2004). The solid line is the model without a dark halo, the dotted line shows the corresponding rotation curve when a dark halo component was included. The rotation curves are practically identical. *Lower panel*: expected number of spiral arms in the radial range where spiral structure can be seen. The dotted curve is again for the model with a dark halo included.

Resolution problem again

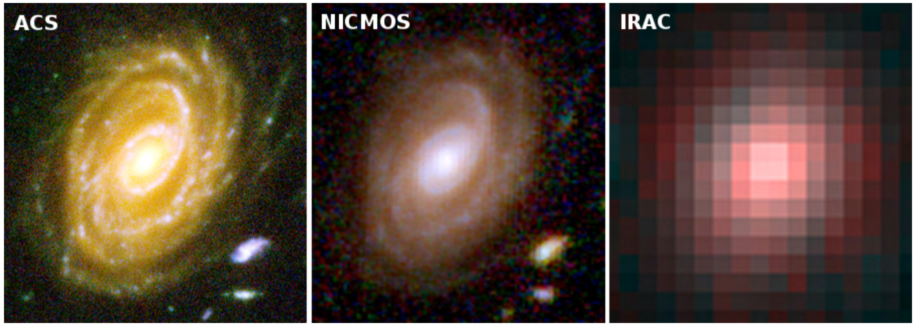

Pixel 0.049 arcsec

Pixel 1.2 arcsec

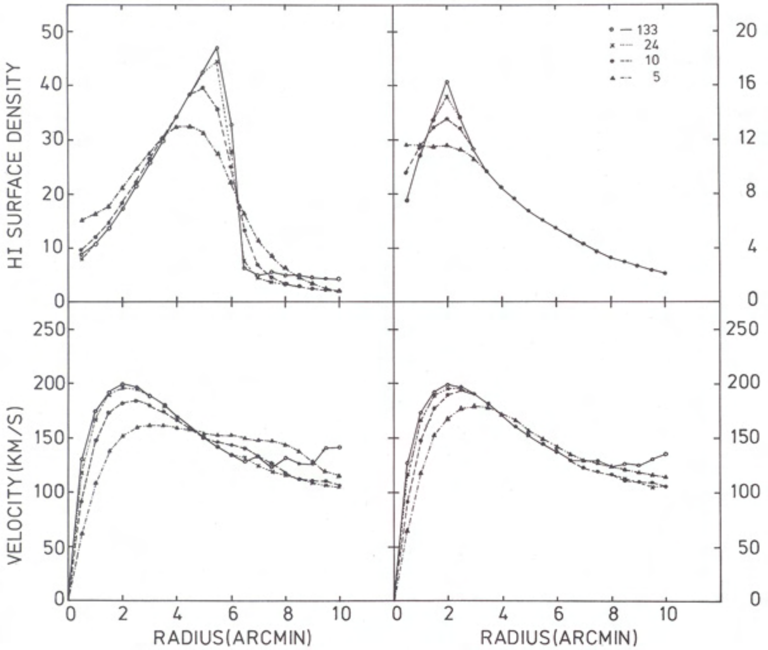

Bosma (1978)

For a good rotation curve better have radius/beamsize large (>7 at least, better 15)

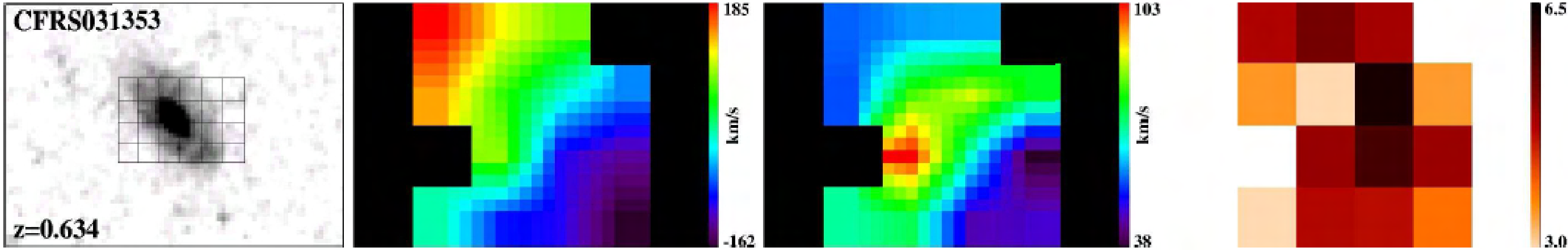

Giraffe – VLT : 0.52 arcsec/pixel; typically 8hrs/exposure

Flores et al. 2006

Tully - Fisher results at z = 0.6

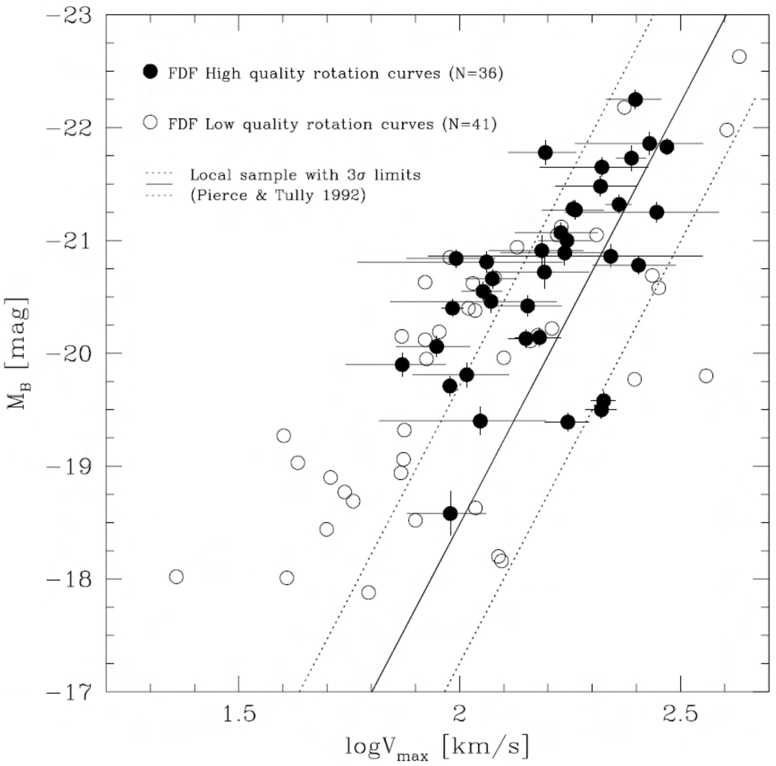

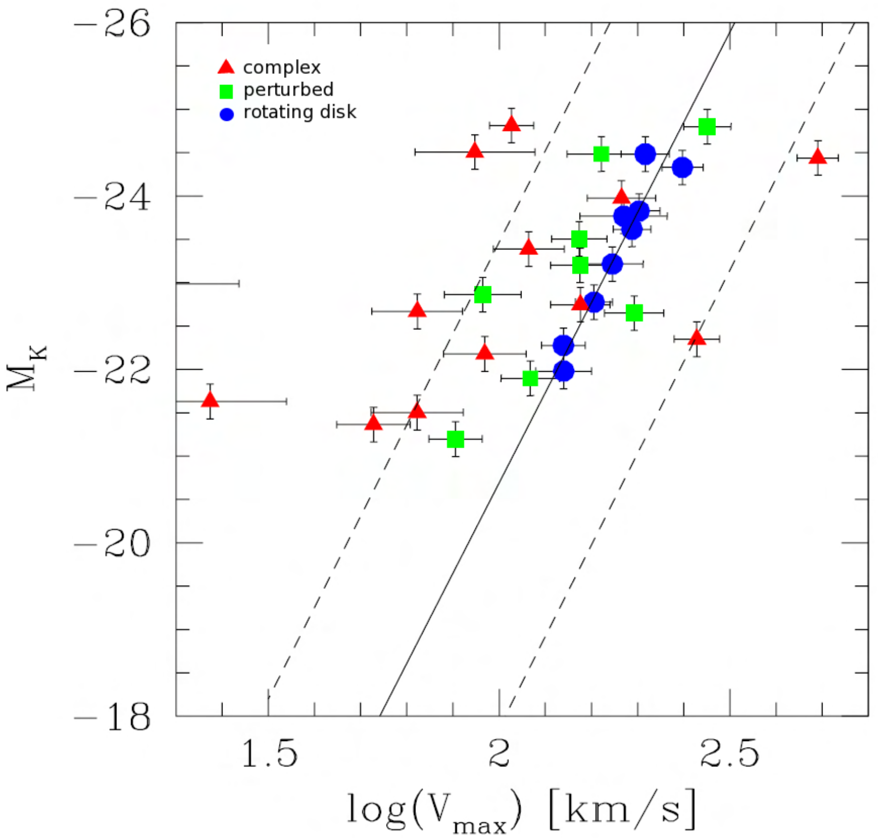

Böhm et al. 2004
use FORS

Flores et al. 2006
use GIRAFFE

the 2-D data allow
sorting out the rotators

SKA – 100x more sensitive as VLA

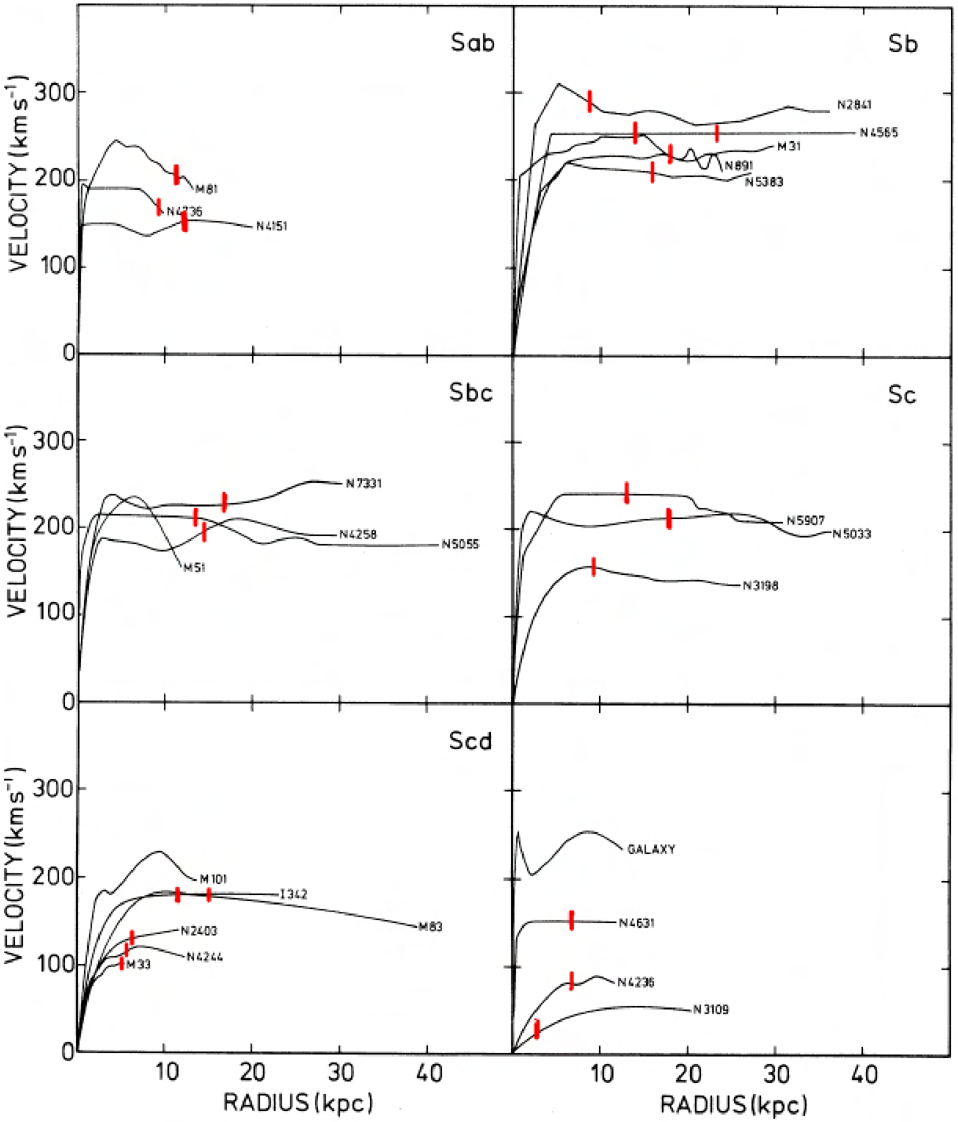

Bosma 1978 FIG. 3. Rotation curves of 25 galaxies of various Hubble types.

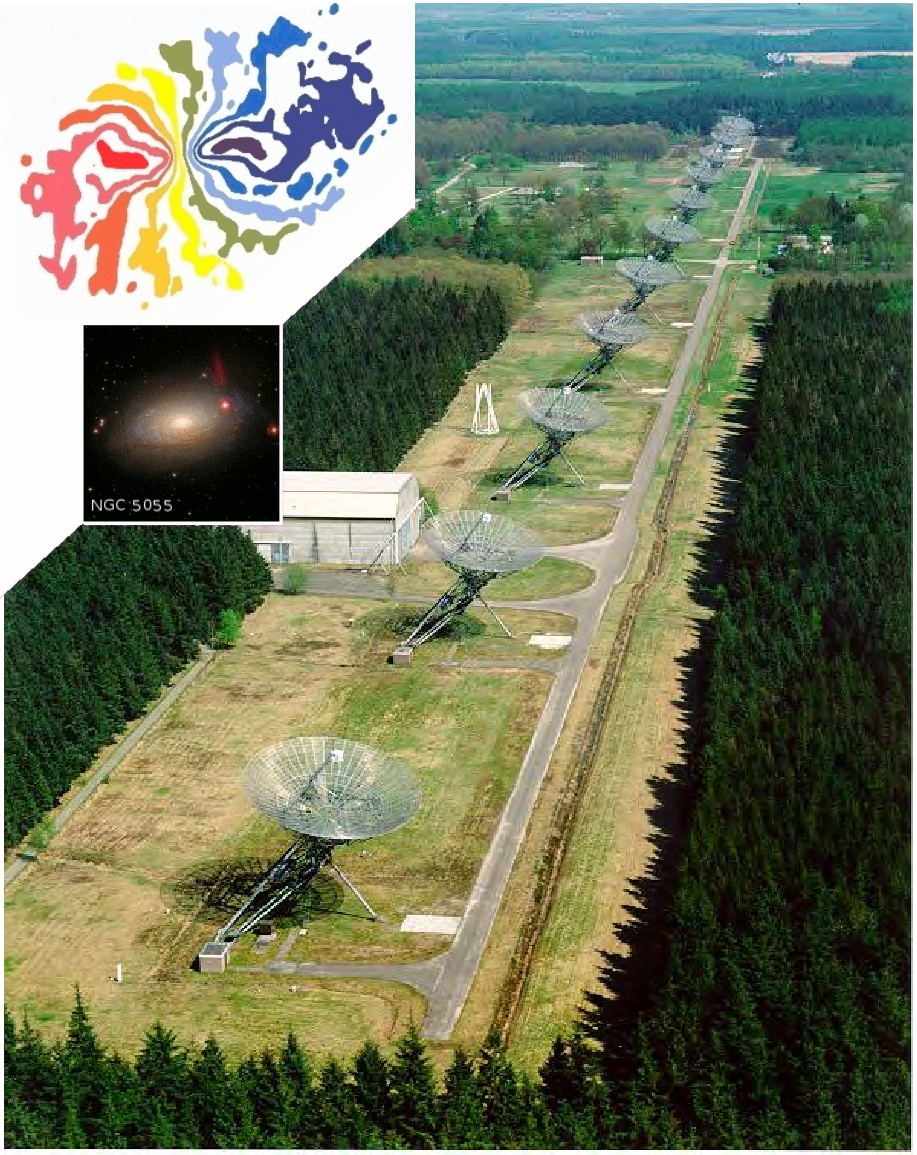

SKA – 100x

SKA will image galaxies such as M81 and N5055 at z ~ 1

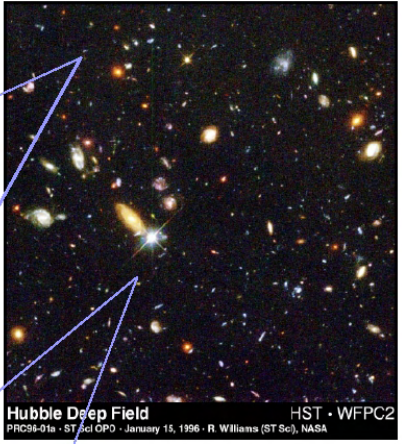

But at a small ratio Radius/Beamsize !

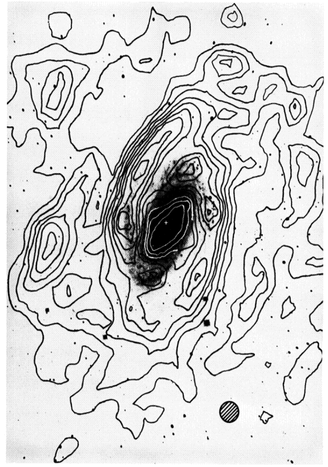

FIG. 4.—The contours of equal H I density of fig. 3 superposed on a photograph of M81 (courtesy Dr. A. G. Smith)

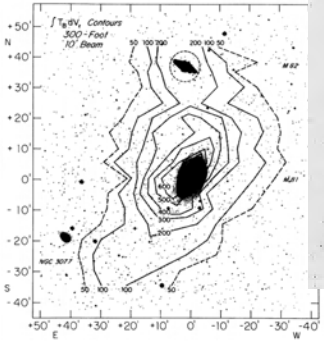

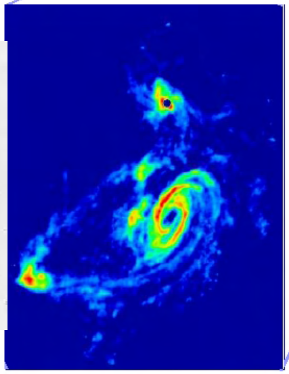

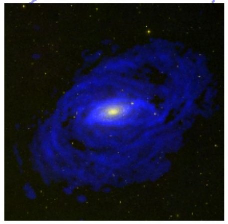

Van der Hulst et al. 2004

Detection limits for HI emission with SKA[a]

z	Frequency (MHz)	$T_{\rm sys}$[b] (K)	Angular[c] resolution (arcsec)	Linear resolution (kpc)	SB dimming (mag)	Luminosity distance (Gpc)	Lookback time (Gyr)	HI mass[d] limit ($M_\odot$)
0.2	1183.67	50.4	0.52	1.7	0.796	0.972	2.41	6.1×10^8
0.5	946.94	51.4	0.65	4.0	1.486	2.825	5.02	8.7×10^8
1.0	710.20	53.8	0.87	7.0	3.026	6.640	7.73	2.7×10^9
1.5	568.16	57.5	1.09	9.3	4.000	11.02	9.32	7.2×10^9
2.0	473.47	62.7	1.31	11.1	4.796	15.75	10.32	1.5×10^{10}
2.5	405.83	69.6	1.52	12.5	5.469	20.72	11.00	2.6×10^{10}
3.0	355.10	78.3	1.74	13.6	6.052	25.87	11.48	4.3×10^{10}
3.5	315.64	89.3	1.96	14.6	6.566	31.15	11.83	6.7×10^{10}

[a] Assuming $t = 12$ h, $A_e/T_{\rm sys} = 20000$, 2 polarizations and 70% of A_e within 100 km.

[b] Including a contribution from Galactic foreground emission assuming $T_{\rm Gal}(f_{\rm MHz}) = 20\left(\frac{408}{f_{\rm MHz}}\right)^{2.7}$ K.

[c] Fixed array geometry assumed so that resolution scales with wavelength.

[d] Assuming 5 rms and 100 km s^{-1} profile width. At $z = 0.2$ and $z = 0.5$ the galaxies are assumed resolved so here the flux has been added over 8.5 and 1.5 beams respectively.

SKA – 100x more sensitive as VLA

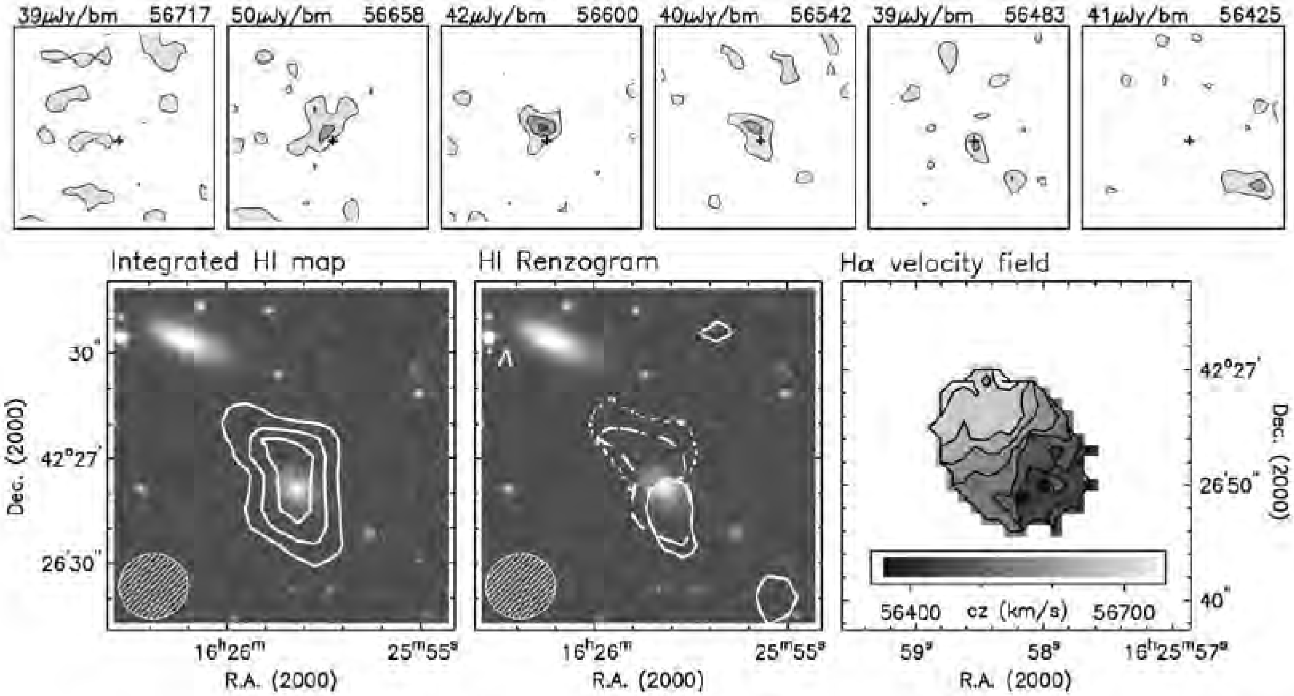

Fig. 8. Atomic Hydrogen detected in Abell 2192 at $z = 0.1887$. Upper panels: individual channel maps from the VLA datacube. The rms noise and Heliocentric velocity are noted above each panel. Lower left: Total HI map. The contours coincide with the position of an inclined barred late-type galaxy. Lower middle: contours from the three channel maps plotted on top of each other; solid: cz = 56483 km/s, dashed: cz = 56542 km, dotted: cz = 56600 km/s. Lower right: Hα velocity field of the optical counterpart obtained with the PMAS IFU spectrograph at the 3.5m telescope on Calar Alto. There is excellent correspondence between the HI and Hα recession velocities, confirming the HI detection. From Verheijen and Dwarakanath (in preparation).

Verheijen &
Dwarakanath

EVLA can already do some of it at lower z
JWST will have IFU with resolution 3000

SKA is also a redshift machine

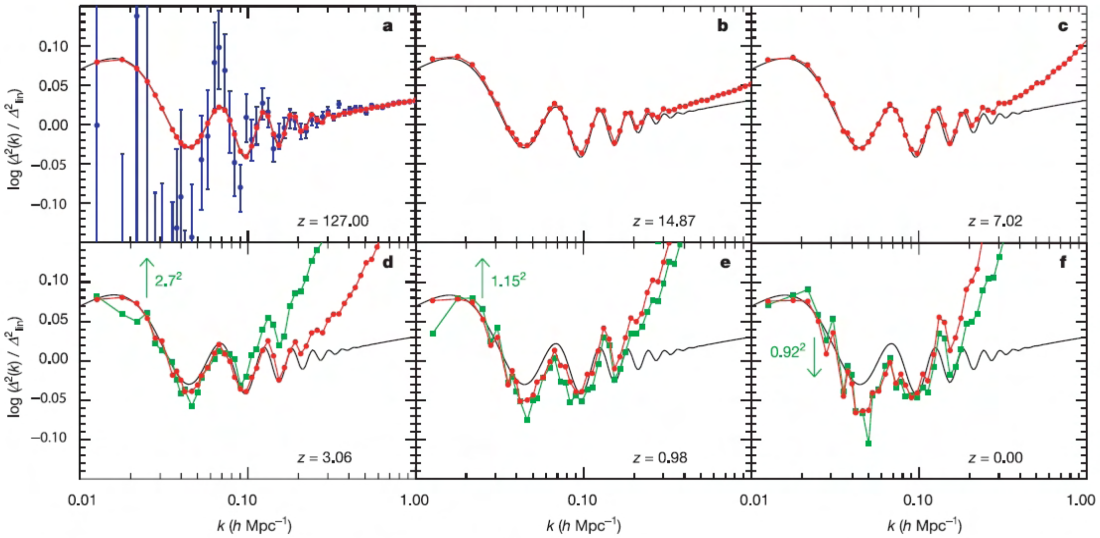

Figure 6 | Power spectra of the dark matter and galaxy distributions in the baryon oscillation region. a–f, All measurements have been divided by a linearly evolved, CDM-only power spectrum $\Delta^2_{\rm lin}$ (ref. 40). Red circles show the dark matter, and green squares the galaxies. Blue symbols give the actual realization of the initial fluctuations in our simulation, which scatters around the mean input power (black lines) owing to the finite number of modes (error bars give the 1-σ scatter around the mean power in each bin). Because linear growth preserves relative mode amplitudes, we correct the power in each bin to the expected input power and apply these scaling factors at all other times. **d**, At $z = 3.06$, galaxies with stellar mass above $5.83 \times 10^9 h^{-1} M_\odot$ and space-density of $8 \times 10^{-3} h^3\,{\rm Mpc}^{-3}$ were selected. Their large-scale density field is biased by a factor $b = 2.7$ with respect to the dark matter (the galaxy measurement has been divided by b^2). **f**, At $z = 0$, galaxies brighter than $M_{\rm B} = -17$ and a space density higher by a factor of ~7.2 were selected. They exhibit a slight antibias of $b = 0.92$. **e**, The corresponding numbers for $z = 0.98$ are $M_{\rm B} = -19$ and $b = 1.15$.

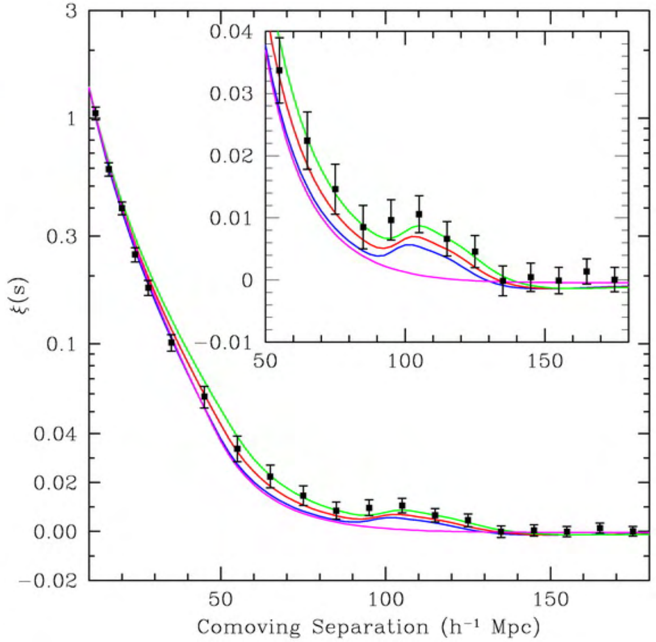

C.A. Blake et al. / New Astronomy Reviews 48 (2004) 1063–1077

Baryonic acoustic oscillations :
predicted in simulations,
found in SDSS Eisenstein et al.
can be done with SKA to
constrain dark energy parameters

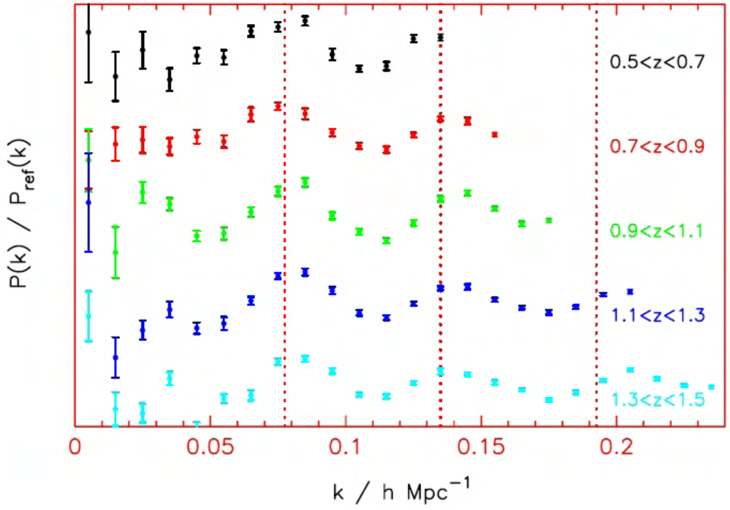

Radio-FIR correlation and redshift ?

Carilli & Yun 1999

$$S_{\mathrm{radio}} = 4 \times 10^{28} \left[\frac{(1+z)^{1+\alpha_{\mathrm{radio}}}}{4\pi D_L^2}\right] \left[\frac{\nu_{\mathrm{radio}}}{1.4\ \mathrm{GHz}}\right]^{\alpha_{\mathrm{radio}}}$$

synchotron emission of relativistic electrons accelerated in supernovae remnant shocks

$$\times\ \mathrm{SFR\ ergs\ cm^{-2}\ s^{-1}\ Hz^{-1}},$$

$$S_{\mathrm{submm}} = 1 \times 10^{28} \left[\frac{(1+z)^{1+\alpha_{\mathrm{submm}}}}{4\pi D_L^2}\right] \left[\frac{\nu_{\mathrm{submm}}}{350\ \mathrm{GHz}}\right]^{\alpha_{\mathrm{submm}}}$$

thermal dust emission

$$\times\ \mathrm{SFR\ ergs\ cm^{-2}\ s^{-1}\ Hz^{-1}},$$

$$\alpha_{1.4}^{350} = -0.24 - [0.42 \times (\alpha_{\mathrm{radio}} - \alpha_{\mathrm{submm}}) \times \log(1+z)]$$

Radio-FIR correlation and redshift ?

Klein et al. 1988

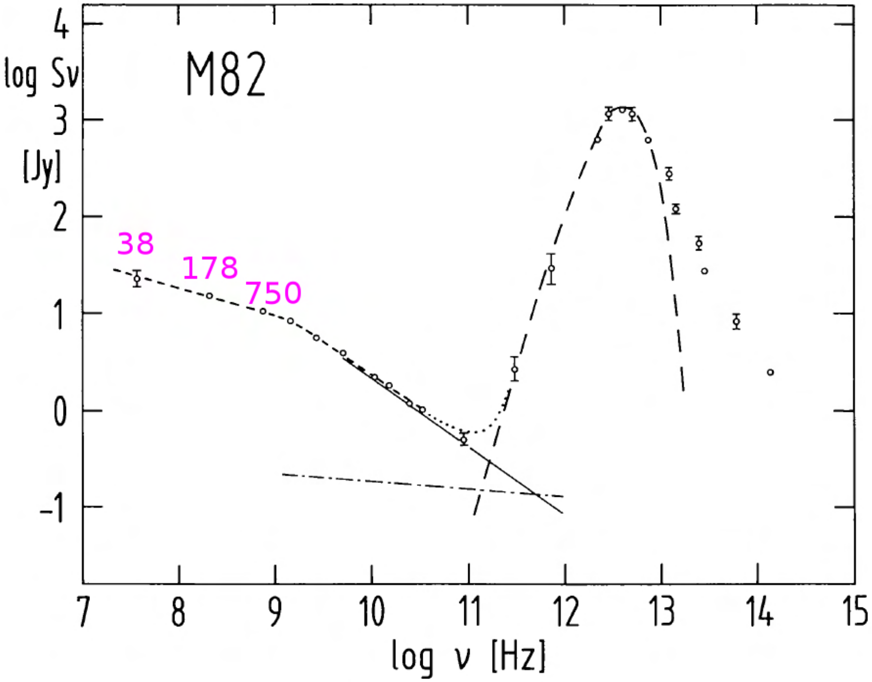

Photometric redshifts by SED fitting

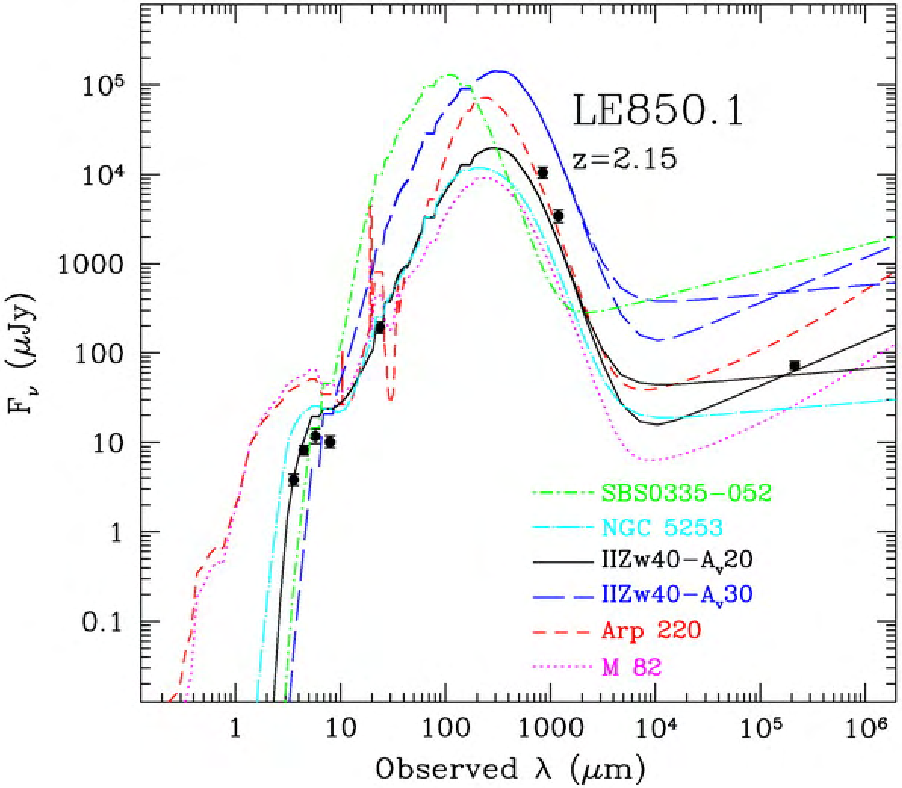

At LOFAR frequencies, spectral index has changed

Radio-FIR correlation inside galaxies

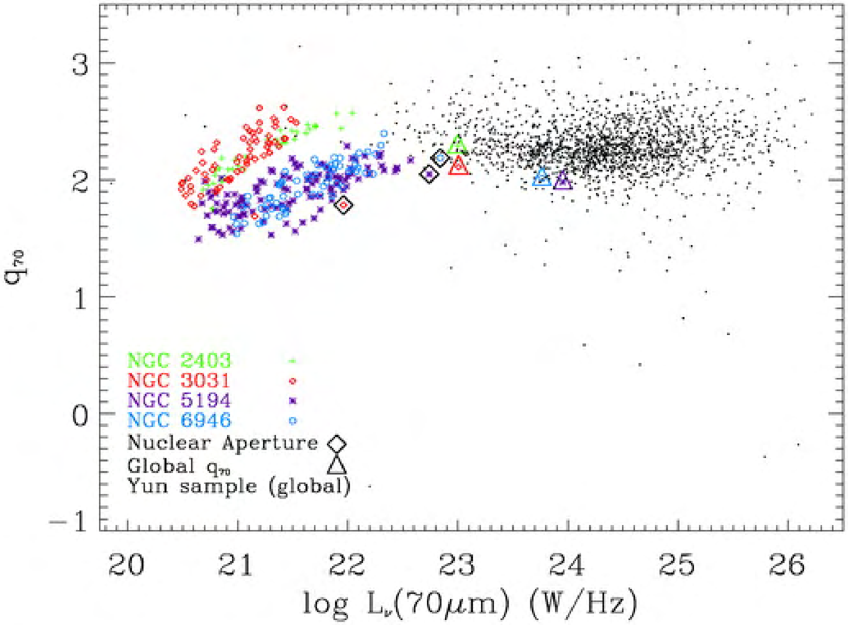

Murphy et al. 2006
using Spitzer (SINGS)

Low q-values could mean early phase starburst
Roussel et al. 2004

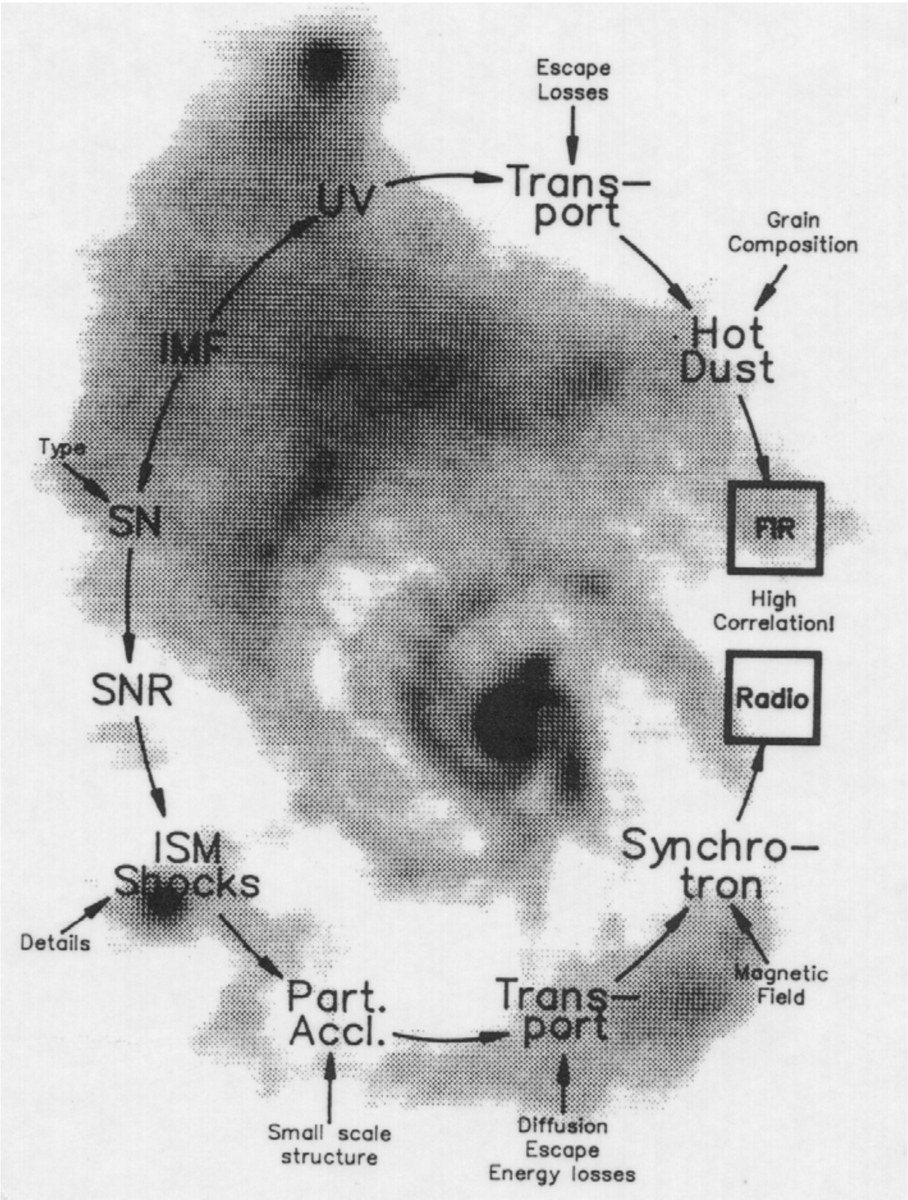

Radiocontinuum in galaxies

Israel & Maloney 1990 57.5 MHz

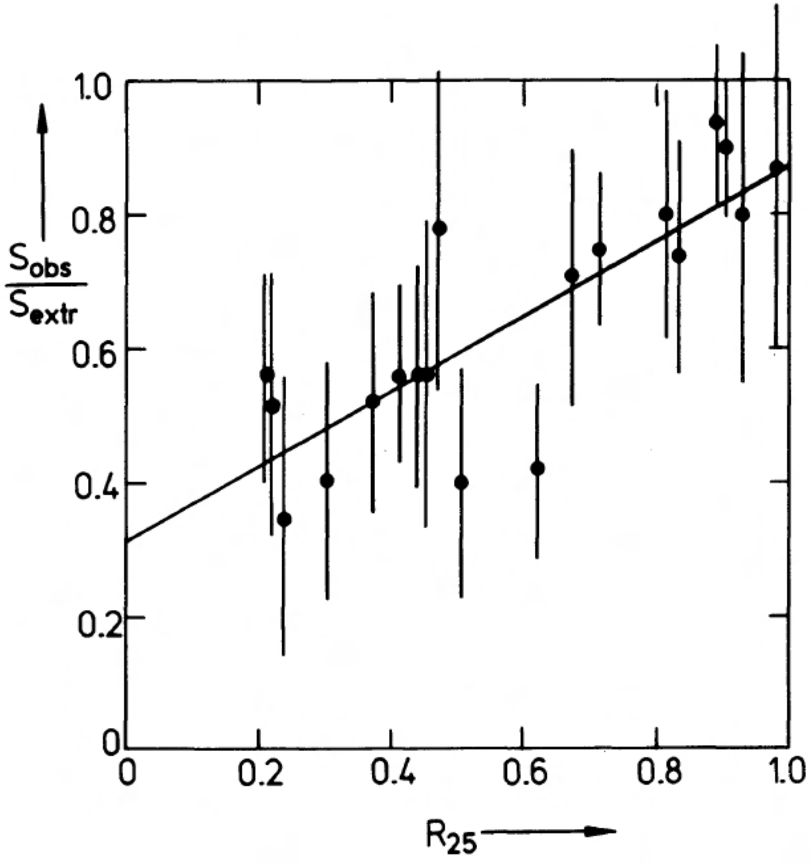

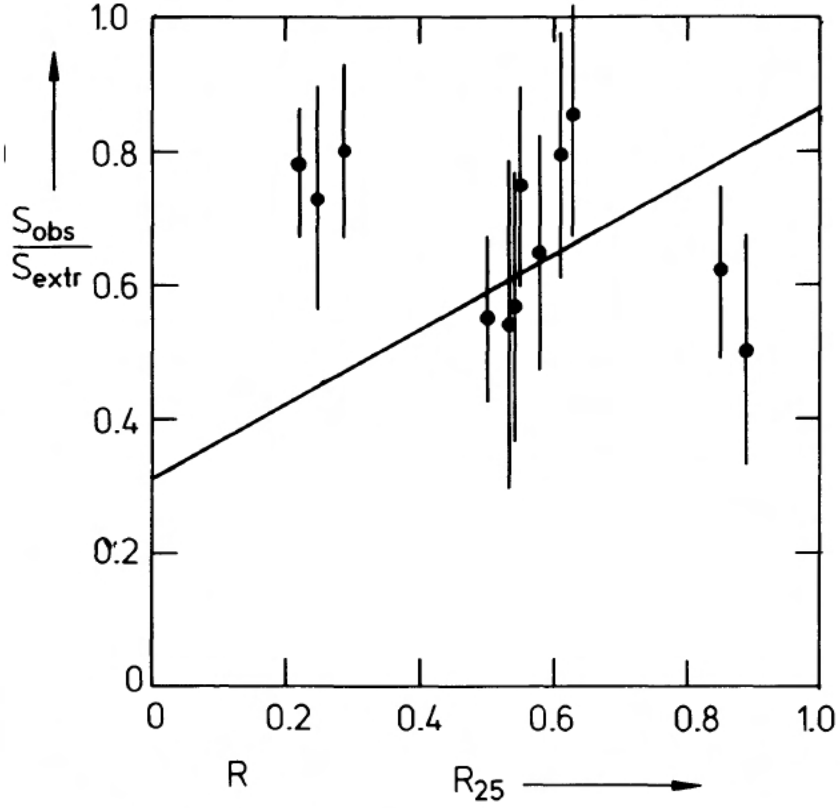

FIG. 3.—Same as Fig. 2*a*, but for galaxies with strong central component ($S_{cen}/S_{tot} > 0.1$ at 1400 MHz). The linear regression fit from Fig. 2*a* is added for comparison.

increasing free-free absorption of non-thermal emission with increasing tilt

but complications if central component is strong

Radiocontinuum in galaxies

Beck et al.

- dynamos
- shocks
- outflows

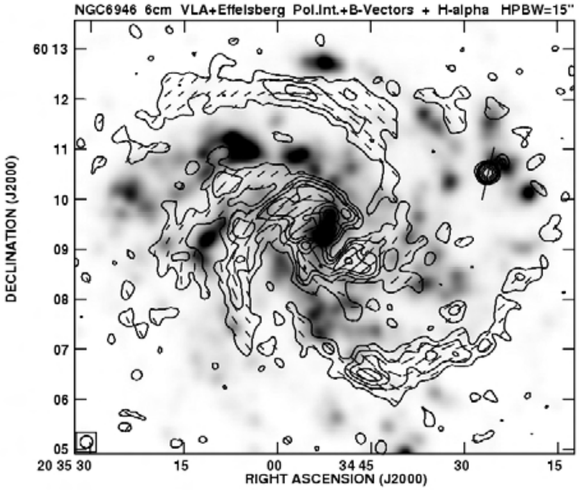

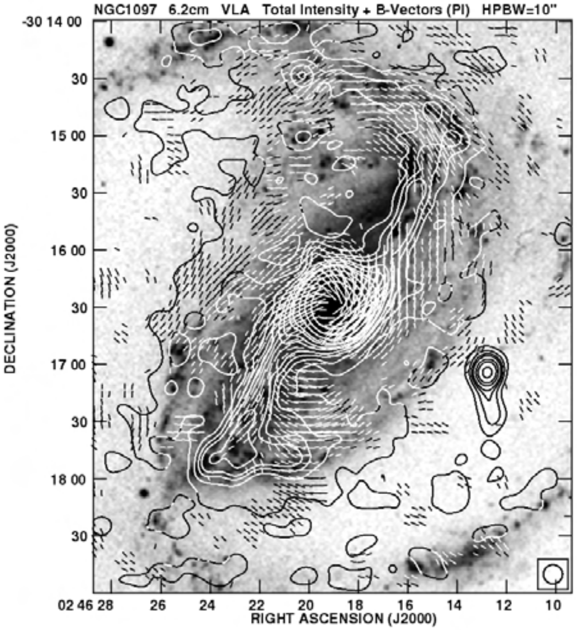

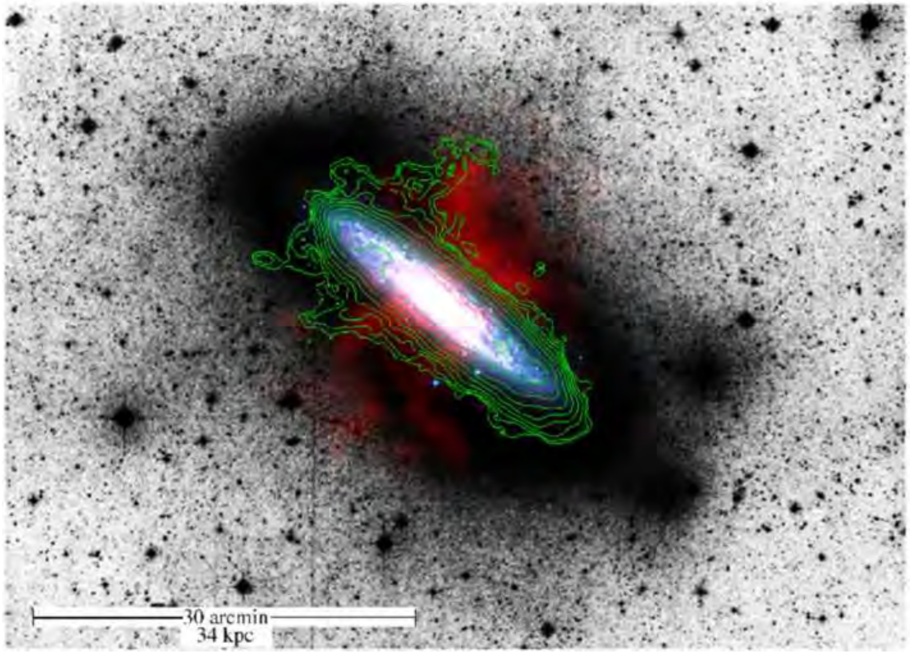

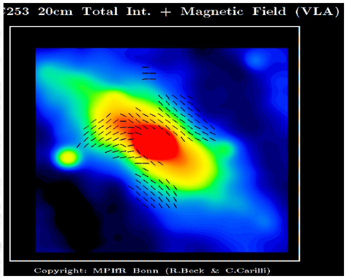

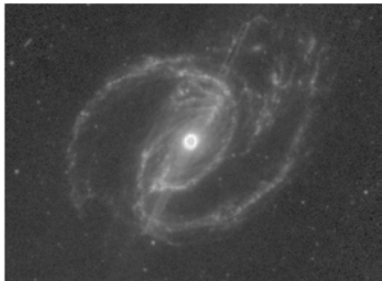

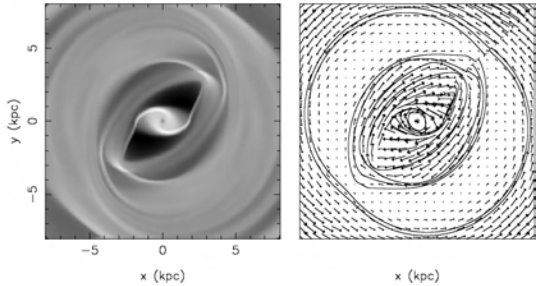

Indirectly back to dark matter ??

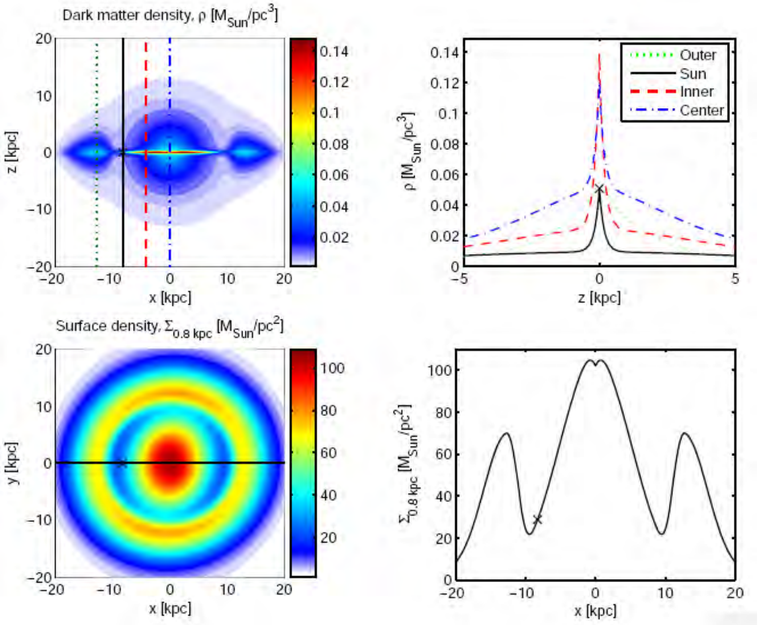

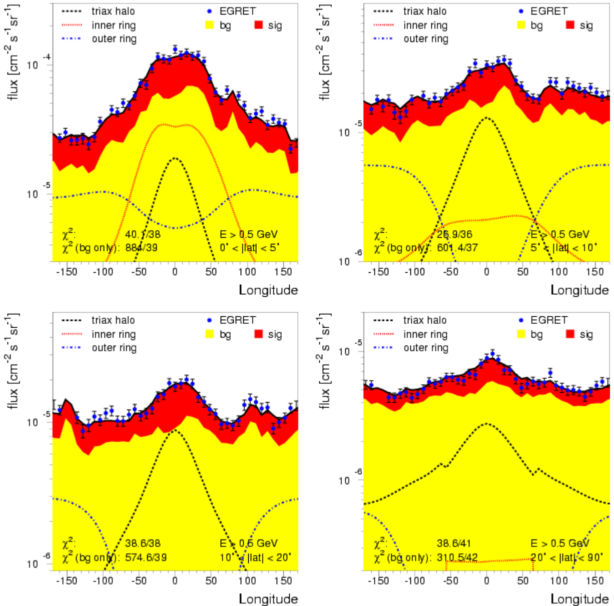

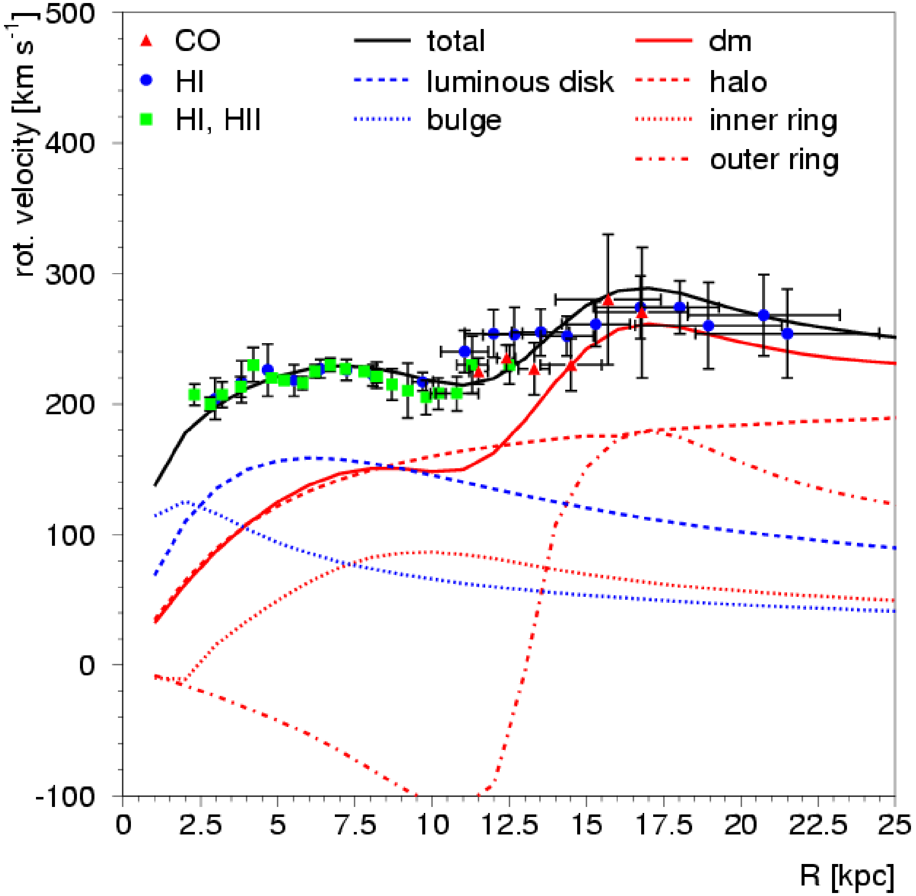

Fit to EGRET data

de Boer et al. 2005

Bergström et al. 2006

Galaxies with LOFAR

1. Resolution matters

2. SKA will have fundamental impact on galaxies and cosmology studies

3. LOFAR explores little studied frequency range

4. Complex physics

5. LOFAR science could lead to better SKA participation (better technical understanding; ask how you will train those who will be the SKA users 10 years from now)

Lensing surveys

Koopmans & Treu (2003)
Koopmans – astro-ph/0511121;
Bolton + K + T (3 papers)